JCB Article

Balancing different types of actin polymerization at distinct sites: roles for Abelson kinase and Enabled

Elizabeth E. Grevengoed,[1] Donald T. Fox,[2] Julie Gates,[3] and Mark Peifer[1,2,3]

[1]Curriculum in Genetics and Molecular Biology, [2]Department of Biology, and [3]Lineberger Comprehensive Cancer Center, University of North Carolina at Chapel Hill, Chapel Hill, NC 27599

The proto-oncogenic kinase Abelson (Abl) regulates actin in response to cell signaling. *Drosophila* Abl is required in the nervous system, and also in epithelial cells, where it regulates adherens junction stability and actin organization. Abl acts at least in part via the actin regulator Enabled (Ena), but the mechanism by which Abl regulates Ena is unknown. We describe a novel role for Abl in early *Drosophila* development, where it regulates the site and type of actin structures produced. In Abl's absence, excess actin is polymerized in apical microvilli, whereas too little actin is assembled into pseudocleavage and cellularization furrows. These effects involve Ena misregulation. In *abl* mutants, Ena accumulates ectopically at the apical cortex where excess actin is observed, suggesting that Abl regulates Ena's subcellular localization. We also examined other actin regulators. Loss of Abl leads to changes in the localization of the Arp2/3 complex and the formin Diaphanous, and mutations in *diaphanous* or *capping protein β* enhance *abl* phenotypes.

Introduction

Morphogenesis is the process by which changes in cell shape, migration, and adhesion mold the body plan of an organism. The dynamic interplay between a cell's actin cytoskeleton and its cortex is at the heart of many of these activities. Although many molecules have been identified that regulate cytoskeletal dynamics or cytoskeletal attachment to cell–cell and cell–matrix adhesive junctions, the mechanisms by which these are integrated are not well understood.

One signaling molecule that regulates cortical actin in response to cell–cell signals is the nonreceptor tyrosine kinase Abelson (Abl; for review see van Etten, 1999). The NH_2-terminal region of Abl is related to the Src family kinases, with SH3 and SH2 domains that mediate protein interactions and a tyrosine kinase domain. In Abl, these are joined by a less highly conserved region to COOH-terminal F- and G-actin binding sites. As a result, cytoplasmic Abl associates with actin filaments (van Etten et al., 1994). Mammalian Abl also localizes to nuclei, where it is activated in response to DNA damage and can trigger apoptosis (for review see Wang, 2000). Interest in Abl was increased by the fact that certain human leukemias are triggered by Bcr-Abl, a chimeric fusion protein with elevated kinase activity (for review see van Etten, 1999). Bcr-Abl localizes to the cytoplasm, suggesting its role in oncogenesis occurs there.

One of Abl's major roles is to regulate actin in response to cell–cell signals (for review see Woodring et al., 2003). In fibroblasts, Abl promotes actin rearrangement in response to both PDGF and cell spreading (Plattner et al., 1999; Woodring et al., 2002). Genetic analyses in mice support a role for Abl and the related, partially redundant kinase Abl-related gene (Arg) in promoting cytoskeletal rearrangements. $abl^{-/-}$ $arg^{-/-}$ double mutants die during embryogenesis with defects in neurulation; mutant neuroepithelial cells have an altered actin cytoskeleton (Koleske et al., 1998). Perhaps the best understood example is the role of *Drosophila* Abl in axon outgrowth during central nervous system (CNS) development (for review see Lanier and Gertler, 2000). Mutations in axon guidance receptors or actin regulators enhanced *abl* CNS phenotypes (for review see Lanier and Gertler, 2000). This led to a model whereby Abl receives signals from axon guidance receptors and influences actin via its effects on proteins like Trio and profilin (for review see Korey and Van Vactor, 2000).

D. Fox and J. Gates contributed equally to this paper.

The online version of this article includes supplemental material.

Address correspondence to Mark Peifer, Dept. of Biology, Coker Hall, CB #3280, University of North Carolina at Chapel Hill, Chapel Hill, NC 27599-3280. Tel.: (919) 962-2271. Fax: (919) 962-1625. email: peifer@unc.edu

Key words: adherens junctions; Arp 2/3; formins; capping protein; cellularization

Abbreviations used in this paper: Abl, Abelson; abl^{M}, *abl* maternal mutant; α-cat, α-catenin; AJ, adherens junction; Arg, Abl-related gene; Arm, Armadillo; *cpb*, *capping protein β*; CNS, central nervous system; Dia, Diaphanous; Ena, Enabled; VASP, vasodilator-stimulated phosphoprotein.

To understand how cytoskeletal changes regulate processes such as axon outgrowth, we must understand the many proteins that regulate actin dynamics (for review see Pollard and Borisy, 2003). For example, the Arp2/3 complex nucleates new actin filaments, forming branches from the sides of preexisting filaments. Formins like yeast Bni1p or fly Diaphanous (Dia) may also nucleate new actin filaments, though their mechanism of action is less clear. Profilin binds actin monomers, preparing them for addition to growing filaments by mediating nucleotide exchange. Capping protein limits polymerization by binding to the barbed end of growing filaments, whereas actin-depolymerizing factor/cofilin severs existing filaments.

Another family of actin modulators, the Enabled/vasodilator-stimulated phosphoproteins (Ena/VASP) (fly Ena and mammalian Mena, Evl, and VASP; for review see Krause et al., 2002), may link Abl action and cytoskeletal regulation. Artificially mistargeting Ena/VASP proteins to the leading edge of migrating fibroblasts or depleting them from this site have opposite effects on both actin polymerization and cell migration (Bear et al., 2000, 2002). Ena/VASP proteins promote the formation of long, unbranched actin filaments. In vitro experiments suggest they do so by binding the barbed end and antagonizing capping protein (Bear et al., 2002).

ena mutations were originally identified as dominant genetic suppressors of *Drosophila abl* (Gertler et al., 1990). Like Abl, Ena regulates the cytoskeleton during axon outgrowth (for review see Korey and Van Vactor, 2000). Furthermore, *Drosophila* Ena is a direct target of Abl kinase (Comer et al., 1998). Mammalian Abl can also bind to and regulate Mena and VASP (Lambrechts et al., 2000; Howe et al., 2002; Tani et al., 2003). Together, these data suggest that Abl negatively regulates Ena, but the mechanism of this negative regulation remains unclear.

Abl and Ena also play roles in epithelial cells (Baum and Perrimon, 2001; Grevengoed et al., 2001), where one of Abl's functions is to regulate the stability of adherens junctions (AJs; Grevengoed et al., 2001). These apical adhesive junctions are organized around transmembrane cadherins, which mediate homophilic adhesion and assemble cortical catenin complexes that anchor the actin cytoskeleton. The association of AJs with actin is essential for their maintenance and for adhesion (Hirano et al., 1992). Ena, Mena, and VASP all localize to epithelial AJs (Vasioukhin et al., 2000; Baum and Perrimon, 2001; Grevengoed et al., 2001). Thus, we sought to distinguish whether Abl's effects on AJs are direct or are mediated via effects on the actin cytoskeleton associated with them, potentially through Ena/VASP.

The early *Drosophila* embryo provides an excellent system in which to examine this question. Early development happens in a syncytium where 14 rounds of nuclear division occur without cytokinesis (for review see Foe et al., 1993; Sullivan and Theurkauf, 1995). During nuclear cycle 10, nuclei migrate to the embryo's cortex and undergo four more synchronous cell cycles, during which dynamic actin rearrangements occur. During interphase, actin forms a microvillar cap above each nucleus (Fig. 1 A, top). As nuclei enter mitosis, actin relocalizes to transient membrane invaginations known as pseudocleavage furrows. These furrows physically separate and anchor adjacent spindles (Fig. 1 A, bottom), and actin is thought to help form and stabilize them. As mitosis ends, furrows retract and caps reform. During interphase of cycle 14, membranes invaginate between each nucleus in a process called cellularization (Fig. 1 B). Actin primarily localizes to the base of the invaginating membrane and is thought to drive invagination. Actin also transiently localizes to microvilli above each nucleus at the onset of cellularization, which disappear over time (Fig. 1 B). AJ proteins localize to pseudocleavage furrows (McCartney et al., 2001) and just apical to actin during cellularization (Thomas and Williams, 1999; Hunter and Wieschaus, 2000). During syncytial stages, Abl localizes to actin caps and to pseudocleavage furrows. During cellularization, Abl localizes to the apicolateral regions of the newly forming cells, and it remains apical during early gastrulation (Bennett and Hoffmann, 1992). Thus, Abl is positioned to potentially regulate either actin or AJ proteins. The distinct localizations of actin and AJ proteins during syncytial divisions and cellularization allowed us to address the effects of Abl depletion on each.

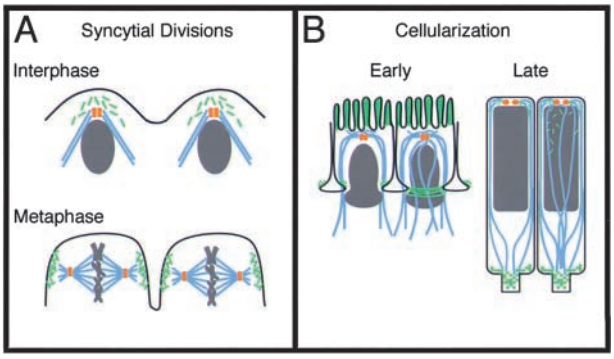

Figure 1. **Cytoskeletal rearrangements during syncytial development and cellularization.** Actin, green; microtubules, blue; centrosomes, orange; membrane, black; nuclei, gray. (A) Syncytial divisions. (B) Cellularization. See text for details. Adapted from Foe et al. (1993).

Here, we demonstrate a role for Abl in regulating actin organization in early embryos. We show that Abl prevents inappropriate actin polymerization by regulating Ena localization. In Abl's absence, Ena accumulates ectopically at the apical cortex. This shifts the balance of actin polymerization, inducing the formation of excess surface microvilli, whereas actin lining the pseudocleavage and cellularization furrows is reduced. Arp2/3 and the formin Dia are recruited to ectopic actin structures stimulated by Ena. We explored the role these regulators of actin polymerization might play in the generation of the *abl* phenotype. We also found that mutations in *capping protein* β (*cpb*) enhance *abl* phenotypes, consistent with the hypothesis that Ena is a capping protein antagonist. Our data suggest that Abl is a key cytoskeletal regulator that helps balance distinct types of actin polymerization at different sites within the cell.

Results

Abl is required for proper actin organization during syncytial development and cellularization

Embryos that are both maternally and zygotically mutant for *abl* (abl^{MZ}) have defects in morphogenesis (Grevengoed et al., 2001). abl^{MZ} mutants also have multinucleate cells. To

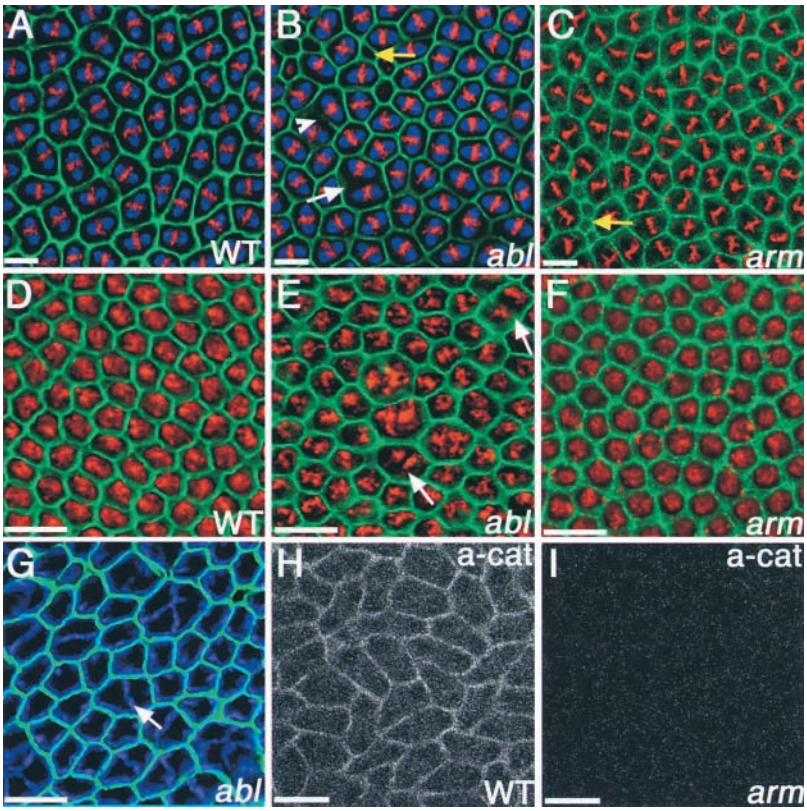

Figure 2. ***abl^{M}* mutants, unlike *arm^{XP33}* mutants, have defects in pseudocleavage and cellularization furrows.** F-actin/junctions in green (A, B, D, E, and G, phalloidin; C and F, junctions labeled with anti-phosphotyrosine) and DNA (propidium iodide) in red. A, B, and G: microtubules in blue. (A–C) Metaphase, syncytial division. (A) Wild-type. (B) *abl^{M}*. Some pseudocleavage furrows are absent (white arrow), whereas others are disintegrating (arrowhead). When nuclei collide, they are removed from the cortex, leaving behind pseudocells with no nuclei (yellow arrow). (C) *arm^{XP33}* maternal mutant. Pseudocleavage furrows are not disrupted, although some nuclei have been removed from the cortex (yellow arrow). (D–F) Cellularization. (D) Wild-type. (E) *abl^{M}*. Some furrows are missing (arrows), resulting in multinucleate cells. (F) *arm^{XP33}*. No multinucleate cells are apparent. (G) *abl^{M}*. Each nucleus is still surrounded by a microtubule basket (arrow). (H and I) α-cat, syncytial divisions. (H) Wild-type. (I) *arm^{XP33}*. Although pseudocleavage furrows are present (C), α-cat no longer localizes there. Experiments were done at 25°C. Bars, 10 μm.

determine why, we examined the early stages of development when cells form. Unless noted, experiments were performed on embryos whose mothers' germlines were homozygous for the protein-null allele *abl^{4}* (Bennett and Hoffmann, 1992) and whose fathers were *abl^{4}* heterozygous. As most zygotic transcription initiates after cellularization begins, and as our earlier experiments suggest that significant levels of zygotic Abl protein are not made until after the onset of gastrulation (Grevengoed et al., 2001), we refer to all of these embryos as maternal *abl* mutants *(abl^{M}*; half are also zygotically *abl* mutant).

We visualized F-actin and nuclei during the syncytial divisions and cellularization. During mitosis of the syncytial divisions in wild-type embryos, actin localizes to pseudocleavage furrows (Fig. 1 A and Fig. 2 A). Thus, each spindle is surrounded by an actin-lined furrow, preventing adjacent spindles from colliding. We observed defects in pseudocleavage furrows of *abl^{M}* mutants. Some furrows are absent (Fig. 2 B, white arrow), whereas others appear to be breaking down (Fig. 2 B, arrowhead). These defects in pseudocleavage furrows sometimes lead to spindle collision, resulting in abnormal mitoses. Abnormal nuclei were removed into the interior of the embryo, leaving behind smaller pseudocells (Fig. 2 B, yellow arrow).

Immediately after the syncytial divisions, furrows again extend between each nucleus during cellularization. In wild-type embryos, images taken at the plane of the nuclei during mid-cellularization reveal a uniform distribution of actin around each nucleus (Fig. 2 D). *abl^{M}* mutants have defects in cellularization furrows, with multiple nuclei surrounded by a single actin ring (Fig. 2 E, arrows). Most multinucleate cells have normal microtubule baskets surrounding each nucleus (Fig. 2 G, arrow). Although some defects in cellularization could reflect the abnormal nuclei generated by nuclear collisions during the syncytial stages, we believe that most do not, as severely defective nuclei should have been removed. We also observed defects in cellularization in *abl^{1}* maternal and zygotic mutants (unpublished data; *abl^{1}* encodes a truncated protein lacking the COOH-terminal actin-binding region; Bennett and Hoffmann, 1992). We focus on *abl^{4}*, as it is a protein-null mutation (Bennett and Hoffmann, 1992).

The defects in Fig. 2 illustrate the mildest phenotype of *abl^{M}* mutants, as *abl^{4}* is cold sensitive (Table I). At 18°C, the defects in cellularization furrows become much more widespread, affecting many, if not most, forming cells (Table I and Fig. 3). We used this sensitivity to vary the severity of the phenotype analyzed. In this analysis, we did not observe two clear phenotypic classes that might represent maternally and zygotically mutant versus paternally rescued embryos, and thus, we suspect that paternal rescue is not effective at the early stages of development that we examined. However, it remains possible that paternal rescue could partially alleviate early phenotypes in the embryos that receive a wild-type paternal chromosome, as it can the later effects of maternal *abl* loss (Grevengoed et al., 2001).

As some kinase-independent functions of Abl have been identified (Henkemeyer et al., 1990; Wang et al., 2001), we investigated whether Abl kinase activity is required during cellularization. To do so, we generated females whose germlines were *abl* mutant and were heterozygous for either a wild-type or a kinase-dead Abl transgene (Henkemeyer et al., 1990; the crosses required to generate these females mean that only half carry the transgene, and thus all progeny are maternally *abl* mutant, but only 50% carry the Abl transgene maternally).

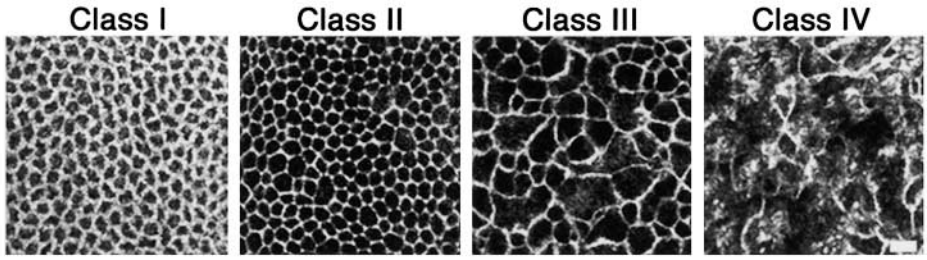

abl^4/abl^4 X $abl^4/+$ at 25°C	15%	55%	28%	2%
abl^4/abl^4 X $abl^4/+$ at 18°C	5%	16%	62%	17%

Figure 3. ***abl*^{M} mutants are cold sensitive.** Embryos labeled to visualize F-actin were ranked by phenotypic severity. Class I: virtually wild-type with no multinucleate cells. Class II: isolated multinucleate cells. Class III: many multinucleate cells, resulting in patches of actin loss. Class IV: severe actin disruption. Percentage of progeny in each class at 25°C vs. 18°C are indicated. These phenotypic classes are also used in Table I. Bar, 10 μm.

We compared the degree of disruption of cellularization furrows to that seen in *abl*^{M} mutants. One copy of the wild-type transgene strongly rescued the *abl*^{M} cellularization phenotype, but the kinase-dead transgene did not (Table I), suggesting that Abl's kinase activity is required during cellularization.

Thus, *abl*^{M} mutants have defects in furrows that form during two distinct developmental processes that resemble one another in two ways: actin plays a role in furrow formation and stabilization (for review see Sullivan and Theurkauf, 1995), and AJ proteins localize to both types of furrows (Thomas and Williams, 1999; Hunter and Wieschaus, 2000; McCartney et al., 2001). In epithelia, Abl plays a role in AJ maintenance (Grevengoed et al., 2001), and thus we considered two hypotheses to explain the defects observed in actin-based furrow formation. First, Abl might regulate AJ proteins in early embryos, such that in the absence of Abl their localization or function was disrupted, leading to defects in actin. Alternatively, Abl might more directly influence the actin cytoskeleton by regulating proteins such as Ena.

AJ proteins are not Abl's targets during early embryogenesis

To test the first hypothesis, we analyzed embryos mutant for the essential AJ protein *armadillo* (*arm*) to determine if they exhibit a phenotype similar to that of *abl*^{M} mutants. We used *arm*^{XP33}, a strong hypomorphic allele, to generate *arm* maternal mutants (null *arm* alleles disrupt oogenesis). Previously, we found that *arm*^{XP33} maternal mutants have defects in spindle attachment to the cortex during syncytial divisions; the resulting nontethered nuclei are removed from the embryo's periphery (Fig. 2 C, arrow; McCartney et al., 2001). However, *arm*^{XP33} embryos do not have defects in pseudocleavage furrows (Fig. 2 C; McCartney et al., 2001). We also analyzed *arm*^{XP33} maternal mutants for defects in cellularization, and found no evidence for multinucleate cells (Fig. 2 F). Although it is possible that some residual Arm function may be present that masks effects on actin, we observed no detectable α-catenin (α-cat) in pseudocleavage (Fig. 2, compare H with I) or cellularization furrows (Cox et al., 1996) of *arm*^{XP33} mutants, suggesting that AJs are substantially disrupted.

We also analyzed the localization of AJ proteins in *abl*^{M} mutants. During the extended germband stage and dorsal closure, Arm and α-cat levels are uniformly reduced at cell–cell junctions in *abl*^{MZ} mutants (Grevengoed et al., 2001). In contrast, Arm and α-cat levels are not uniformly reduced in either pseudocleavage furrows or basal junctions (unpublished data). The only change we saw in their localization

Table I. **Tests of genetic interactions between *abl* and actin regulators**

Parental genotype	Class I	Class II	Class III	Class IV	*n*
	%	%	%	%	
abl^4glc × $abl^4/+$ at 25°C	15	55	28	2	64
abl^4glc × $abl^4/+$ at 18°C	5	16	62	17	65
TnAblWT/+;abl^4glc × $abl^4/+$ at 18°C[a]	36	25	33	6	48
TnAblK-N/+;abl^4glc × $abl^4/+$ at 18°C[a]	6	27	55	12	43
$ena^2$10/+;abl^4glc × $abl^4/+$ at 18°C[a]	32	24	28	16	68
$sop2^{Q25st}/+$;abl^4glc × $abl^4/+$ at 25°C[a]	11	48	37	4	80
$sop2^{Q25st}/+$;abl^4glc × $abl^4/+$ at 18°C[a]	11	24	46	19	52
$dia^2/+$;abl^4glc × $abl^4/+$ at 25°C[a]	11	13	45	30	50
$dia^2/+$;abl^4glc × $abl^4/+$ at 18°C[a]	4	12	42	42	49

Class I, least severe. Class IV, most severe. Compare Table I with pictures in Fig. 3. glc, germline clone; TnAblWT, wild-type Abl transgene; TnAblK-N, kinase-dead Abl transgene (Henkemeyer et al., 1990).
[a]Only half of the mothers carried the indicated Abl transgene, or were heterozygous for *ena*, *sop2*, or *dia* (see Materials and methods for details).

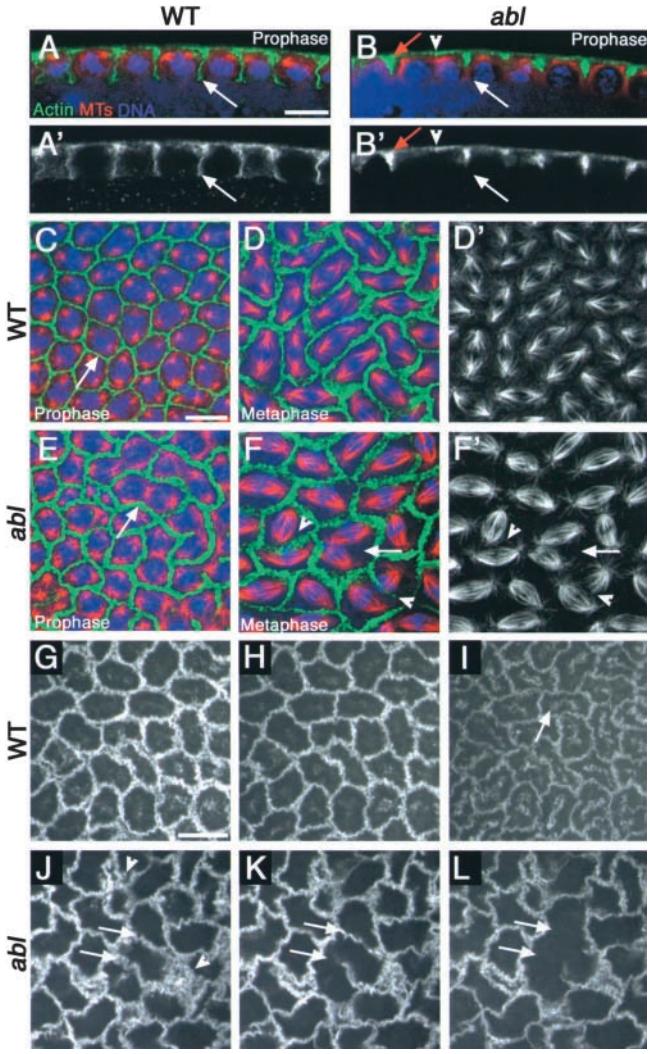

Figure 4. **Elevated apical actin localization in *abl*^{M} mutants is accompanied by furrow defects.** (A–F′) Syncytial divisions. F-actin (phalloidin) in green, microtubules in red, and DNA (DAPI) in blue. (A′ and B′) Actin alone. (D′ and F′) Microtubules alone. (A–B′) Cross section. (C–F′) Apical surface view. (A, A′, B, B′, C, and E) Prophase. (D, D′, F, and F′) Metaphase. (A and A′) Wild-type. Pseudocleavage furrows (arrow). (B and B′) *abl*^{M}. Excess actin in the apical-most region of the furrow (red arrow). Missing furrow (arrowhead). Incomplete furrow (white arrow). (C, D, and D′) Wild-type. (C) Prophase. Pseudocleavage furrows (arrow) are thin and uniform. (D and D′) Metaphase. Furrows thicken as they change shape, and spindles remain separated. (E) *abl*^{M}. Prophase. The apical-most region of the furrows (arrow) are thicker and more filamentous (compare with C). (F and F′) *abl*^{M}. Metaphase. Furrow defects lead to spindle collisions both where furrows are absent (arrow) and occasionally where some actin remains (arrowheads). (G–L) Surface view: living embryos expressing moesin-GFP, filmed during syncytial divisions. (G–I) Wild-type (Video 1, available at http://www.jcb.org/cgi/content/full/jcb.200307026/DC1). Prophase (G), metaphase (H), anaphase/telophase (I). Pseudocleavage furrows remain intact. Arrow, Cytoplasmic actin that may be relocalizing to caps. (J–L) *abl*^{M} (Video 2). Prophase (J), metaphase (K), anaphase/telophase (L). Some furrows break down at anaphase onset (arrows). Excess apical actin (arrowheads). Experiments done at 18°C. Bars, 10 μm.

was likely indirect—when actin-based pseudocleavage or cellularization furrows were absent in *abl*^{M} mutants, neither AJ proteins nor any other normal constituents of these furrows localized there (unpublished data). Together, these data suggest that AJ components are not direct targets of Abl during syncytial stages or cellularization.

abl^{M} mutants have excess apical actin, whereas actin in furrows is depleted

Given these results, we examined whether Abl acts more directly on the actin cytoskeleton. We performed these experiments at 18°C, using the cold sensitivity of *abl*^{4} to enhance its phenotypic severity. During prophase, wild-type pseudocleavage furrows uniformly extend below the nuclei (Fig. 4, A and A′). During metaphase and later in mitosis, wild-type furrows retract somewhat, but still invaginate past the depth of each spindle (unpublished data). In *abl*^{M} mutants, we observed dramatic changes in actin localization; less actin was found in pseudocleavage furrows, whereas excess actin was found apically. We observed defects in pseudocleavage furrows as early as prophase (Fig. 4, B and B′). Furrows were sometimes absent (Fig. 4, B and B′; arrowhead), and furrows that did form were variable in depth, never invaginating to the depth of wild-type furrows (Fig. 4, B and B′; white arrow). Furrow defects were also seen in metaphase (Fig. 4 F). The absence of furrows during metaphase in *abl*^{M} mutants often led to spindle collision (Fig. 4, F and F′; arrow). Even when actin localized to pseudocleavage furrows, microtubules from adjacent spindles sometimes collided (Fig. 4, F and F′; arrowheads), suggesting that either furrows are incomplete or they fail to invaginate deep enough to prevent spindle collision (Fig. 4, B and B′). In contrast to the loss of actin from pseudocleavage furrows, *abl*^{M} mutants accumulate elevated levels of actin in the apical-most region of all of the furrows (Fig. 4, B and B′; red arrows), giving the actin in this region a thicker, more filamentous appearance (Fig. 4, compare C with E, arrows). Thus, although we only observe complete failure in furrow formation in a subset of *abl*^{M} pseudocells, actin localization along the length of pseudocleavage furrows is dramatically altered in all of them.

We also visualized F-actin in real time, imaging wild-type and *abl*^{M} mutants expressing the actin-binding domain of moesin fused to GFP (Kiehart et al., 2000). In wild-type syncytial embryos, actin forms a cap above each interphase nucleus during the syncytial phase. As nuclei enter mitosis, actin relocalizes to pseudocleavage furrows and remains there until anaphase/telophase, when it diminishes from the furrows and reaccumulates in caps (Fig. 4, G–I; Video 1, available at http://www.jcb.org/cgi/content/full/jcb.200307026/DC1). Our wild-type movies also showed some "intracellular" actin accumulation as actin leaves the furrows (Fig. 4 I, arrow), which may be actin relocalizing to caps. Using this type of analysis, we found that in *abl*^{M} mutants, some furrows form properly but are torn apart during anaphase (Fig. 4, J–L; arrows). This does not always lead to nuclear fallout, as many pseudocells in which furrows failed generated normal-size actin caps in the next interphase (Video 2). Thus, some furrows that form in *abl*^{M} mutants appear not to be as strong as in the wild-type, presumably as a result of changes in depth or actin localization we observed in our fixed images.

abl^{M} mutants have similar defects during cellularization, exhibiting excess apical actin at the expense of some cellulariza-

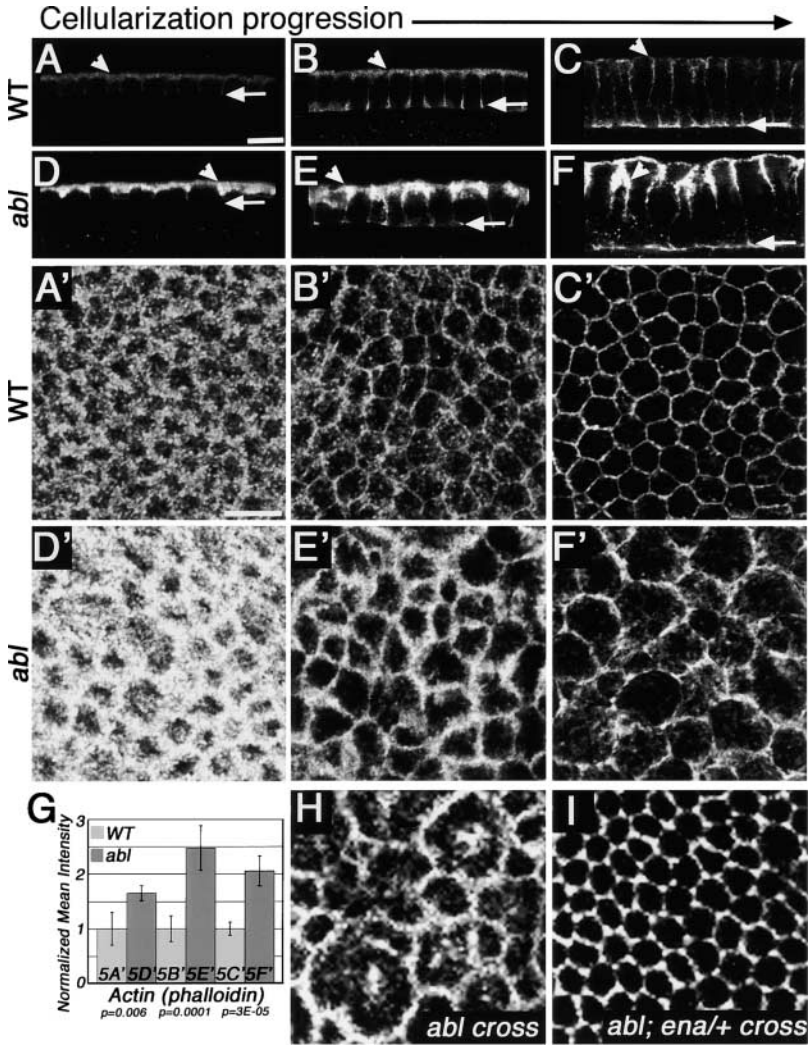

Figure 5. ***abl*^{M} mutants exhibit aberrant apical actin accumulation during cellularization.** Embryos labeled with phalloidin to visualize F-actin. (A–F) Cross sections, progressive stages of cellularization. Arrowheads, cortical region. Arrows, cellularization front. (A′–F′) Apical surface views of the same embryos. (A–C′) Wild-type. (A and A′) Onset of cellularization. Actin localizes to cortical microvilli, and begins to accumulate in cellularization furrows. (B and B′) Mid-cellularization. Actin at the cellularization front becomes more pronounced. (C and C′) Late cellularization. Actin is strongly enriched at the cellularization front and accumulates at uniform low levels along the lateral membrane. (D–F′) *abl*^{M}. Highly elevated levels of actin accumulate in the apical region throughout cellularization (arrowheads). This may correspond to the excess microvilli in Fig. 7. (G) Quantitation of the change in actin accumulation in the apical region of the lateral membranes during cellularization. MetaMorph® was used to quantitate the phalloidin fluorescence intensity of 10 equivalent regions in the indicated stage-matched wild-type and mutant panels. The wild-type mean was normalized to 1.0, and the SDs and statistical significance (as assessed by a two-tailed, homoscedastic *t* test) are indicated. (H and I) Representative embryos from mothers whose germlines were *abl* mutant (H) or whose germlines were *abl* mutant and also *ena* heterozygous (I). These embryos illustrate the most common phenotype from each cross, as described in more detail in Table I. Experiments done at 18°C. Bars, 10 μm.

tion furrows. In wild-type embryos during early cellularization, newly forming furrows have a "fuzzy" distribution of actin along the cortex (Fig. 5 A, arrowhead; Fig. 5 A′), which may reflect the microvilli seen at this time (see below). As cellularization progresses, actin primarily localizes to the base of the invaginating furrow (Fig. 5 C, arrow). The actin remaining apically forms very crisp rings (Fig. 5 C′). *abl*^{M} mutants have dramatic differences in actin localization throughout cellularization. Many cellularization furrows do not form properly (Fig. 2 and Fig. 3). In parallel, actin localization to the apicolateral region of the furrows is elevated relative to the wild type at the onset of cellularization (Fig. 5 D, arrowhead), and this persists throughout the process (Fig. 5, D–F′). The excess apical actin has a highly filamentous nature, with filopodial-like projections emanating from cell borders (Fig. 5, E′ and F′). We quantitated the differences in F-actin accumulation in the apical region of the lateral membranes between the forming cells in wild-type and *abl*^{M} mutants using MetaMorph®. Apical F-actin levels were from 1.6 to 2.5 times higher in *abl*^{M} mutants (Fig. 5 G; a more comprehensive set of fluorescence quantitation data is in Table S1, available at http://www.jcb.org/cgi/content/full/jcb.200307026/DC1). Total levels of actin in the cell are not altered (Fig. 6 G), suggesting that the primary effect is on actin localization.

Reduction in the Ena dose strongly suppresses the *abl*^{M} defects in cellularization

Because of the dramatic alterations in the actin cytoskeleton of *abl*^{M} mutants, we next investigated the role of molecules involved in actin regulation or pseudocleavage furrow formation. First, we examined Ena, a known substrate of Abl and modulator of actin dynamics (for review see Krause et al., 2002). Ena misregulation plays a critical role in *abl* phenotypes in later embryos (Gertler et al., 1990; Grevengoed et al., 2001). To test whether Ena misregulation contributed to the defects in cellularization, we generated females whose germlines are homozygous mutant for *abl* and also heterozygous for *ena*, thus reducing the maternal contribution of Ena by half. We found that *ena* heterozygosity strongly suppresses the cellularization phenotype of *abl*^{M} mutants (Table I). Most suppressed embryos exhibit far fewer multinucleate cells and less apical actin (embryos illustrating the most frequent phenotype in each cross are presented in Fig. 5, H and I). The level of suppression was similar to that conferred by the wild-type *abl* transgene (Table I).

In *abl*^{M} Ena accumulates at highly elevated levels at the cortex

These data suggest that Ena misregulation contributes to the cellularization defects in *abl* mutants. Next, we explored the

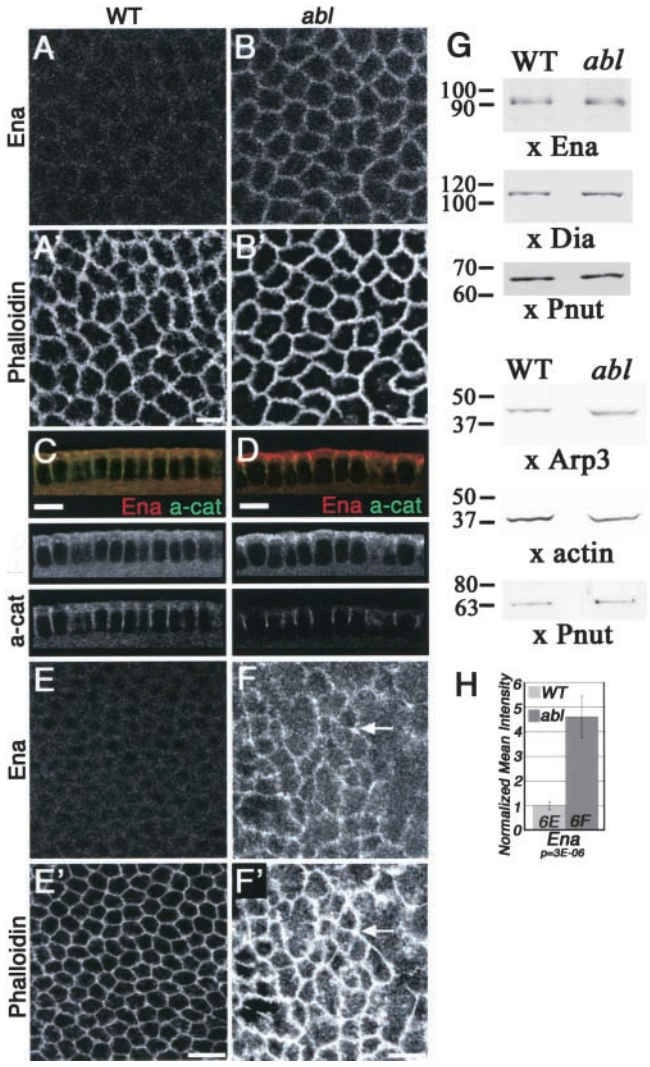

Figure 6. **Ena accumulates in the apical region of *abl*^{M} mutants.** Embryos double-labeled with anti-Ena (A, B, E, and F) and phalloidin (A′, B′, E′, and F′), or anti-Ena (C and D, red) and anti-α-cat (C and D, green). (A–B′) Prophase, syncytial division. (A and A′) Wild-type. (B and B′) *abl*^{M}. Ena is enriched in pseudocleavage furrows. (C and D) Cross section, mid-cellularization. (C) Wild-type. (D) *abl*^{M}. Ena is dramatically enriched along the apical cortex. (E–F′) Apical surface, mid-cellularization. (E) Wild-type. (F) *abl*^{M}. Ena is enriched at the apical ends of furrows (arrows). (G) Levels of Ena, actin, Arp3, and Dia are unchanged in *abl*^{M} mutants. Whole-embryo extracts from wild-type and *abl*^{M} syncytial/cellularizing embryos were run on SDS-PAGE and immunoblotted with antibodies to Ena, Dia, Arp3, actin, and Peanut (Pnut; the loading control). (H) Quantitation of the change in Ena accumulation in the apical region of the lateral membranes during cellularization in *abl*^{M} mutants, as in Fig. 5. Experiments done at 18°C. Bars, 10 μm.

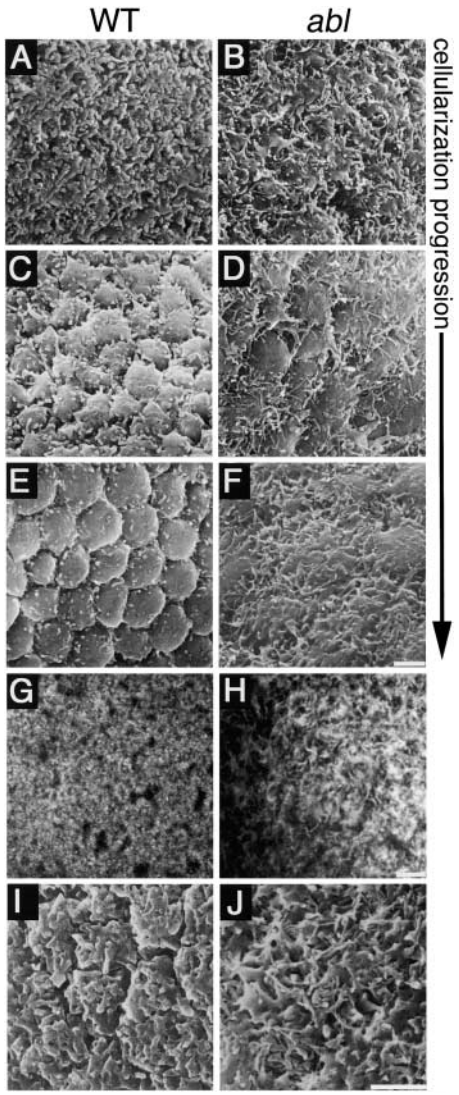

Figure 7. **Apical surface microvilli persist and elongate in *abl*^{M} mutants.** (A–F, I–J) Scanning EM of cellularizing (A–F) or syncytial (I and J) embryos. (A and B) Onset of cellularization. (C and D) Mid-cellularization. (E and F) End of cellularization. (A, C, and E) Wild-type. Apical microvilli diminish over time and are gone at the end of cellularization. (B, D, and F) *abl*^{M}. Microvilli are longer at the onset of cellularization and persist and elongate as development proceeds. (G and H) Stills of living embryos at cellularization onset expressing moesin-GFP. (G) Wild-type (Video 3, available at http://www.jcb.org/cgi/content/full/jcb.200307026/DC1). Microvilli are short. (H) *abl*^{M}. Microvilli are elongated (see Video 4). (I and J) Prophase, syncytial division. (I) Wild-type. (J) *abl*^{M}. Experiments done at 18°C. Bars: 5 μm (A–F, I, and J), 10 μm (G and H).

mechanism by which Abl modulates Ena because this remains largely unknown. We compared the levels and localization of Ena during the syncytial divisions and cellularization in wild-type embryos and *abl*^{M} mutants. In wild-type embryos, Ena is present at low levels throughout the cytoplasm during both the syncytial divisions and cellularization, with the only striking feature being its exclusion from nuclei (Fig. 6, A, C, and E). However, in *abl*^{M} mutants, Ena localization is drastically altered: during syncytial divisions Ena is enriched at the apex of pseudocleavage furrows (Fig. 6 B), and during cellularization Ena is enriched along the apical cortex (Fig. 6, D and F), and further concentrated at apical cell junctions (Fig. 6 F, arrow). These are precisely the regions where we observed altered actin localization (Fig. 5; Fig. 6, B′ and F′). We quantitated these differences during cellularization using MetaMorph®, and found that Ena fluorescence at the apical region of the lateral membranes between the forming cells was elevated three- to fivefold in *abl*^{M} mutants (Fig. 6 H; a more comprehensive set of fluorescence quantitation data is in Table S1, available at http://www.jcb.org/cgi/content/full/jcb.200307026/DC1). To determine whether

Abl regulates overall Ena levels or simply regulates its localization, we compared the total levels of Ena present in wild-type and abl^M mutant syncytial/cellularizing embryos. We saw no change in Ena protein levels in abl^M mutants (Fig. 6 G), suggesting that Abl primarily regulates Ena localization.

abl^M mutants have accentuated actin-based microvilli

During the course of our work, Bear et al. (2002) found that forced mistargeting of Ena/VASP proteins to the leading edge of cultured mammalian fibroblasts promoted the formation of long, unbranched actin microfilaments in lamellipodia. We hypothesized that the elevated Ena levels at the cortex observed in abl^M mutants might alter actin in a similar fashion. Therefore, we used scanning EM to analyze the actin-based filopodial/microvillar projections present on the cortex of cellularizing embryos (cellularization stage was determined by cross sectioning embryos, allowing us to visualize both the depth of the cellularization furrow and the surface microvilli). In the wild type at the onset of cellularization, the embryo surface is covered with short actin-based microvilli (Fig. 7 A; Turner and Mahowald, 1979). These microvilli diminish in length and number as cellularization progresses (Fig. 7, C and E; Turner and Mahowald, 1979).

We observed striking differences in the microvilli of abl^M mutants. At early stages of cellularization, wild-type numbers of microvilli are present (Fig. 7 B), but the microvilli are longer than the wild type. This difference becomes more pronounced during later stages of cellularization; when wild-type microvilli are becoming fewer in number and shorter, abl^M mutant microvilli appear to elongate (Fig. 7, compare C and E with D and F). At the completion of cellularization in abl^M mutants, the surface remains covered with elongated microvilli (Fig. 7 F), consistent with our data showing persistence of F-actin in filopodial-like structures emanating from cell borders (Fig. 5, D′–F′).

To visualize the microvilli in living abl^M mutants, we used time-lapse microscopy and moesin-GFP, focusing on the apical-most cortex. In wild-type embryos, we observed short microvilli at the beginning of cellularization (Fig. 7 G; Video 3, available at http://www.jcb.org/cgi/content/full/jcb.200307026/DC1). In contrast, the surfaces of abl^M mutant embryos are covered with longer actin-rich microvillar projections that persist throughout cellularization (Fig. 7 H; Video 4).

We also observed differences in the microvilli in abl^M mutants during syncytial divisions. In wild-type embryos, we assessed cell cycle stage by examining the shape of the pseudocells, which varies through the cell cycle (unpublished data). In most abl^M mutants, the surfaces were so densely covered with microvilli that pseudocell shape was obscured (unpublished data). However, those mutants that we could stage by pseudocell shape had longer, thinner microvilli (Fig. 7, compare I with J). We suspect that this reflects the excess apical actin we observed in fixed images (Fig. 4 E).

Actin nucleators are recruited to aberrant actin structures in abl^M mutants

Our data suggest that in abl^M mutants, the balance of actin polymerization is altered, such that excess actin accumulates apically, whereas less accumulates in pseudocleavage or cellularization furrows. Next, we examined whether the dramatic alteration of actin in abl^M mutants either altered the location or required the activity of other known actin modulators or other proteins that regulate pseudocleavage furrow formation. First, we looked at the localization of a number of different actin-associated proteins or mediators of pseudocleavage furrow formation to determine if their localization is altered in abl^M mutants. We did not see a dramatic effect on most (profilin, Cpb, CAP, anillin, Dah, or Nuf; unpublished data). However, we did see dramatic effects on the localization of two proteins thought to be involved in actin nucleation: Arp3 (Hudson and Cooley, 2002), a component of the Arp2/3 complex, and Dia (Afshar et al., 2000), a formin. There were no significant changes in the total levels of Arp3 or Dia in abl^M mutant syncytial/cellularizing embryos (Fig. 6 G), suggesting that the primary effect is on their localization rather than synthesis or stability.

Both Arp3 and Dia are recruited to the aberrant actin structures that form in abl^M mutants. In wild-type embryos during prophase of the syncytial divisions, Arp3 is excluded from nuclei with weak recruitment to the apical-most region of pseudocleavage furrows (Stevenson et al., 2002; Fig. 8 A). During early cellularization, Arp3 localizes at low levels along the cortex (Stevenson et al., 2002; Fig. 8 C), with only moderate enrichment at cell junctions (Fig. 8 C, arrow), and this does not change significantly during later stages of cellularization (Fig. 8, I and J; left). In contrast, in abl^M mutants the localization of Arp3 to the apical-most region of both pseudocleavage (Fig. 8 B) and cellularization furrows (Fig. 8 D; Fig. 8, I and J, right) is highly elevated. In abl^M mutants, Arp3 has a filamentous appearance that mimics the abnormal distribution of F-actin (Fig. 8, compare D with D′).

Similarly, we found that Dia is recruited to actin structures in abl^M mutants. In the wild type, Dia localizes at low levels to the apical-most region of pseudocleavage furrows (Afshar et al., 2000; Fig. 8 E, arrow). This apical localization is dramatically enhanced in abl^M mutants (Fig. 8 F), and Dia acquires a thicker, filamentous appearance like that of actin (Fig. 8 F′). During wild-type cellularization, Dia primarily localizes with actin at the base of the invaginating cellularization furrow (Afshar et al., 2000; Fig. 8, K and L; arrowheads in left panels), with low levels of Dia at more apical cell borders during cellularization (Fig. 8 G; Fig. 8, K and L, arrows in left panels). This apical localization is substantially elevated in abl^M mutants (Fig. 8 H; Fig. 8, K and L, arrowheads in right panels). We used MetaMorph® to quantitate these differences in Arp3 and Dia localization to the apical region of the lateral membranes between the forming cells during cellularization. Arp3 fluorescence was elevated 2.7–3.8-fold in abl^M mutants, whereas Dia fluorescence was elevated 1.9–3.6-fold (Fig. 8; a more comprehensive set of fluorescence quantitation data is in Table S1, available at http://www.jcb.org/cgi/content/full/jcb.200307026/DC1).

Next, we examined whether mislocalization of the Arp2/3 complex or Dia contributes to the abl^M phenotype. If so, reduction in their dose might suppress the *abl* phenotype, as we observed with *ena*. Thus, we generated females whose germlines were homozygous for mutations in *abl*, half of whom were also heterozygous for null mutations in either

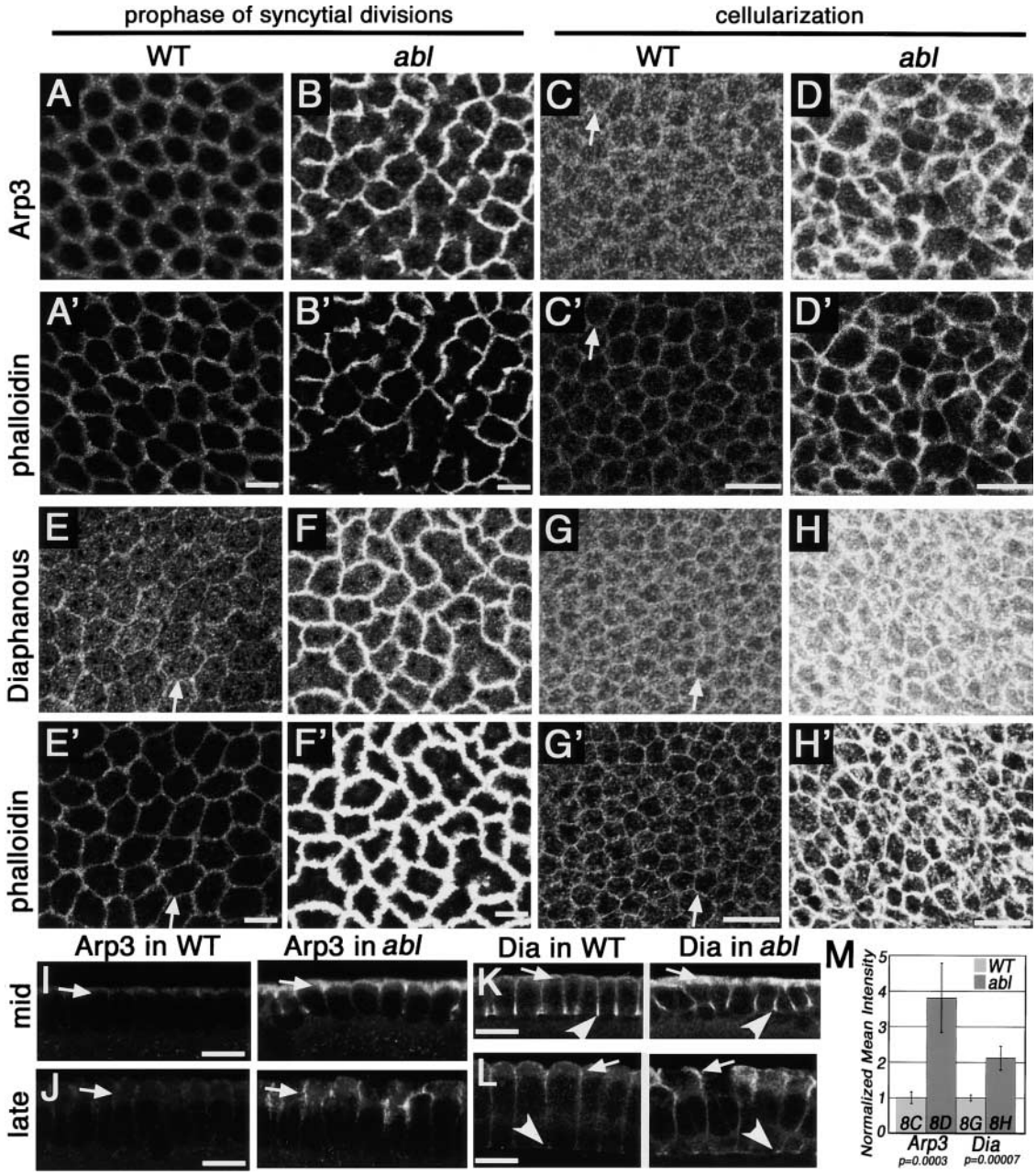

Figure 8. **Arp3 and Dia are recruited to aberrant actin structures in *abl*^{M} mutants.** (A–D′) Embryos double labeled to visualize Arp3 (A–D) and actin (phalloidin; A′–D′). (A–B′) Prophase, syncytial division. (A and A′) Wild-type. Arp3 (A) does not strongly localize with actin (A′) at the apical-most region of pseudocleavage furrows. (B and B′) *abl*^{M}. Arp3 is enriched at apical pseudocleavage furrows (B) along with actin (B′). (C–D′) Cellularization. (C and C′) Wild-type. Arp3 has low level junctional accumulation (arrow). (D and D′) *abl*^{M}. Arp3 (D) and actin (D′) are enriched at cellularization furrows. (E–H′) Embryos double labeled to visualize Dia (E–H) and actin (phalloidin; E′–H′). (E, E′, G, and G′) Wild-type. Low levels of Dia accumulate with actin at prophase pseudocleavage furrows (E and E′, arrows) and cellularization furrows (G and G′, arrows). (F, F′, H, and H′) *abl*^{M}. Dia localization to pseudocleavage (F) and cellularization furrows (H) is dramatically increased. Dia's filamentous distribution mimics actin (F′ and H′). (I and J) Arp3 in cellularizing wild-type or *abl*^{M} mutant embryos, viewed in cross section. (I) Mid-cellularization. (J) Late cellularization. Arrows indicate apical cytoplasm and cell junctions, where elevated levels of Arp3 accumulate in the mutants. (K and L) Dia in cellularizing wild-type or *abl*^{M} mutant embryos, viewed in cross section. (K) Mid-cellularization. (L) Late cellularization. Arrows indicate apical cytoplasm and cell junctions; arrowheads indicate advancing cellularization front. Elevated Dia is seen in the apical cytoplasm of *abl*^{M} mutant embryos. (M) Quantitation of the differences in Arp3 and Dia localization to the apical region of the lateral membranes between the forming cells during cellularization, as in Fig. 5. Experiments done at 18°C. Bars, 10 μm.

the Arp2/3 complex component Arpc1 (*sop2*) or *dia*. Heterozygosity for null alleles of *sop2* or *dia* did not suppress the *abl*^{M} phenotype (Table I). This is consistent with the idea that aberrant localization of Arp2/3 and Dia are not critical for generating the aberrations in actin seen in *abl*^{M} mutants, but, as we were looking for dose-sensitive genetic interactions, it may also be that heterozygosity for *sop2* or *dia* does not reduce the effective dose enough to lead to suppression. However, *dia* heterozygosity significantly enhanced the *abl*^{M} mutant phenotype, suggesting that Dia

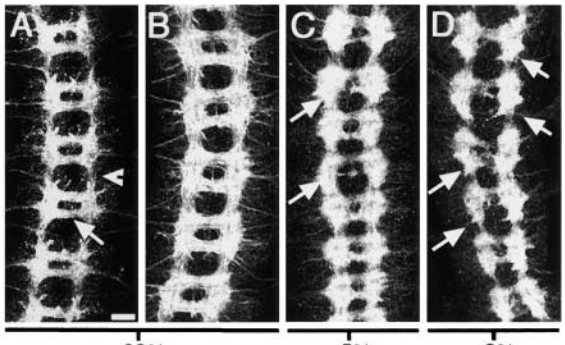

abl/+ X *abl*/+	93%	5%	2%
cpb/+ X *cpb*/+	98	0	2
cpb/+;*abl*/+ X *cpb*/+;*abl*/+	64	15	21
abl/+ X *cpb*/+;*abl*/+	67	13	20
cpb/+;*abl*/+ X *cpb*/+	97	0	3

Figure 9. ***cpb* dominantly enhances *abl*.** Embryos labeled with mAB BP102, revealing all axons. (A and B) Normal early (A) or late (B) CNS, with ladder of longitudinal (arrowhead) and commissural (arrow) axons. (A) Wild-type. (B) abl^4 single mutant. (C and D) Presumptive cpb^{M143};abl^4 double mutants. These illustrate phenotypic classes with minor (C) or major (D) CNS defects, such as gaps in commissures (arrows). Bottom. The percentage of the progeny of each cross that fell into the wild-type, minor defect, or major defect classes. Experiments done at 18°C. Bar, 10 μm.

may counter the effects of Ena misregulation. As Dia is required for formation of pseudocleavage and cellularization furrows (Afshar et al., 2000), reducing its dose may further accentuate the imbalance between apical actin polymerization and that in pseudocleavage and cellularization furrows seen in abl^M mutants.

Mutations in *cpb* strongly enhance *abl*

Based on in vitro analyses, Ena is hypothesized to compete with capping protein for binding to the barbed ends of actin microfilaments, with Ena promoting filament elongation and capping protein prohibiting it (Bear et al., 2002). This model predicts that reducing the level of capping protein might further increase Ena activity, and thus capping protein mutations might enhance *abl* mutants. We generated females whose germlines were homozygous mutant for *abl*, half of which were heterozygous for a hypomorphic mutation in a capping protein subunit, cpb^{M143} (Hopmann et al., 1996). However, these females laid many fewer eggs (potentially due to an enhancement of *abl* effects on oogenesis), precluding an examination of genetic interactions in the early embryo.

Many *abl* genetic interactions were identified by analyzing the CNS of zygotic mutants (for review see Lanier and Gertler, 2000). Thus, we examined zygotic cpb^{M143};abl^4 double mutants, looking for genetic interactions that might affect their viability or the integrity of their CNS. Both cpb^{M143} homozygous and abl^4 homozygous single mutants survive embryogenesis (Table II), and very few of the progeny of these crosses exhibit defects in CNS development (Fig. 9). In contrast, when cpb^{M143}/+;abl^4/+ mothers and fathers were crossed, 20% of the progeny die during embryogenesis (Table II). 15% of the progeny have minor defects in CNS architecture, whereas 21% exhibit more severe CNS defects (Fig. 9). As cpb^{M143};abl^4 double mutants are only 6.25% of the progeny, the frequency of lethality and CNS phenotypes suggested that the mutations might dominantly enhance one another. Further tests suggest that *cpb* is a dominant enhancer of *abl* (Fig. 9 and Table II).

Discussion

Abl regulates Ena localization and thus actin organization

Abl regulates actin polymerization in many settings. Several potential mechanisms have been proposed for this. Mammalian Abl (van Etten et al., 1994) and Arg (Koleske et al., 1998) bind and bundle actin in vitro, suggesting that they may influence actin assembly directly. Abl can bind many cytoskeletal regulators, such as WAVE1 and paxillin, suggesting that it might act as a scaffold to assemble a cytoskeletal regulatory complex (for review see Woodring et al., 2003). Finally, Abl can phosphorylate target proteins, potentially altering their function.

Our genetic analysis suggests that in the early *Drosophila* embryo, the primary means by which Abl influences the cytoskeleton is through Ena. Reducing the Ena dose by half profoundly suppressed abl^M; it is as effective as adding back a wild-type *abl* transgene (Table I). Ena is also a critical target of Abl during embryonic morphogenesis (Gertler et al., 1990; Grevengoed et al., 2001). Although our data suggest that the primary effect of loss of Abl is Ena deregulation, they do not rule out Abl acting on the cytoskeleton by other mechanisms.

The mechanism by which Abl regulates Ena has remained mysterious. Here, we demonstrate that Abl regulates Ena by regulating its intracellular localization. In the absence of Abl, Ena localizes to ectopic sites. Previously, we observed alterations in Ena and actin localization at the leading edge of migrating epidermal cells in *abl* mutants during dorsal closure (Grevengoed et al., 2001). At the time, we did not have a clear explanation for this, but now suspect it suggests that

Table II. **A mutation in *cpb* enhances *abl***

Parental genotype	Embryonic-lethal progeny (%)	*n*
abl^4/+ × abl^4/+	4	177
cpb^{M143}/+ × cpb^{M143}/+	2	269
cpb^{M143}/+;abl^4/+ × cpb^{M143}/+;abl^4/+	20	297
abl^4/+ × cpb^{M143}/+;abl^4/+	20	225
cpb^{M143}/+;abl^4/+ × cpb^{M143}/+	6	269

regulation of Ena localization by Abl may be a more general mechanism. We hypothesize that Abl targets Ena to places where it is needed to modulate actin dynamics, perhaps by excluding it from other sites where Ena activity would be detrimental.

There are many ways in which Abl could restrict Ena localization. Abl's kinase activity is essential, and thus Abl phosphorylation of Ena may restrict its localization by preventing Ena binding to partners that localize to particular cortical sites, or by promoting Ena binding to partners that sequester it in the cytoplasm. Phosphorylation of Ena by Abl in vitro inhibits binding of Ena to SH3 domains (Comer et al., 1998), whereas Mena/VASP phosphorylation by PKA alters binding to SH3 domains and actin (Lambrechts et al., 2000). However, if direct phosphorylation were the only mechanism by which Abl regulated Ena, mutating Ena's phosphorylation sites should create a protein that can no longer be regulated and thus would localize to ectopic sites. Instead, mutation of all of the Abl phosphorylation sites in Ena modestly reduced Ena function (Comer et al., 1998), rather than making it ectopically active as we see in *abl* mutants.

Thus, Abl may regulate Ena by additional mechanisms. Abl may modulate Ena localization and restrict Ena activity by direct binding (this could still require Abl kinase activity, as auto-phosphorylation or phosphorylation of other partners may regulate protein–protein interactions). Abl might sequester Ena in the cytoplasm in an inactive state, or it might recruit Ena to appropriate sites. Alternately, binding of Abl's SH3 domain to the Ena proline-rich region might prevent Ena from binding to other partners, such as profilin (Ahern-Djamali et al., 1999), which might in turn modulate both Ena localization and activity. In thinking about these different possible mechanisms, it is interesting to note that Abl localizes to the actin caps and apical pseudocleavage furrows during syncytial stages and the apical portion of the cellularization furrow (Bennett and Hoffmann, 1992), the precise places where ectopic actin accumulation occurs in its absence. Thus, it is poised to act at this location. Working out the details of the mechanism by which Abl regulates Ena localization will be one of our next challenges.

Our work also provides an in vivo test of the current model for Ena function, and allows us to extend this model. The excess growth of microvilli seen when Ena is ectopically localized in early embryos fits well with work on Ena/VASP function in mammalian fibroblasts, where forced localization of Ena/VASP proteins to the leading edge promotes the formation of long, unbranched filaments (Bear et al., 2002). Ena also localizes to the ends of filopodia and microspikes (Lanier et al., 1999; Vasioukhin et al., 2000; Nakagawa et al., 2001), suggesting that Ena's role in promoting long unbranched actin structures is broadly conserved. Earlier experiments in fibroblasts artificially altered Ena localization. Here, we demonstrate that Ena localization is a normal regulatory point in vivo, and that Abl is a critical player in this process. Finally, in vitro experiments suggested that Ena promotes filament elongation by antagonizing capping protein (Bear et al., 2002). Mutations in *cpb* enhance the effects of mutations in *abl* in the CNS and probably during oogenesis. These data are consistent with Ena and capping protein playing antagonistic roles in vivo, with Abl potentially influencing the outcome of this antagonism.

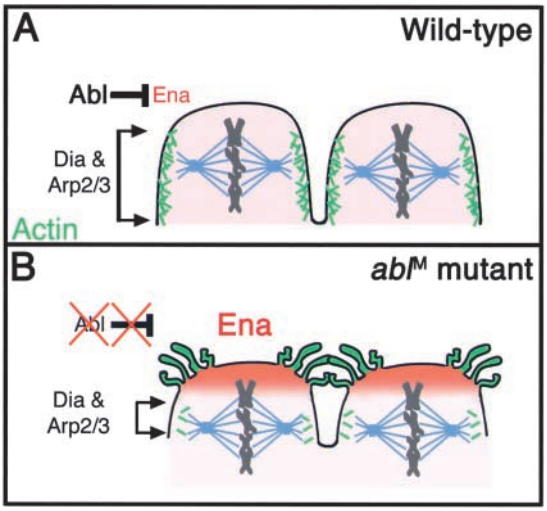

Figure 10. **A model: Abl regulates the site and type of actin polymerization.** (A) Wild-type. Actin accumulates in apical microvilli in interphase and pseudocleavage furrows in mitosis. Abl prevents Ena from accumulating apically during mitosis. Arp2/3 and Dia promote pseudocleavage furrows. (B) abl^M. The balance of actin polymerization is altered. Elevated apical Ena triggers excess actin accumulation in microvilli, depressing actin accumulation in pseudocleavage furrows.

However, Abl and capping protein may also work together independently of Ena in the regulation of actin dynamics.

Cells must balance the activity and localization of different actin regulators

Different actin regulators play fundamentally different biochemical roles (Pollard and Borisy, 2003). Models often picture all of these regulators modulating actin assembly and disassembly at a single site, but of course individual cells target different actin regulators to distinct sites, creating actin structures with diverse functions. Syncytial embryos provide an excellent example (for review see Sullivan and Theurkauf, 1995). During interphase, they assemble actin-based microvillar caps above each nucleus (Fig. 1). As they enter prophase, caps are disassembled and actin polymerization is redirected to the pseudocleavage furrows. This is likely to require new machinery (Fig. 10 A): both Arp2/3 (Stevenson et al., 2002) and the formin Dia (Afshar et al., 2000) are required for pseudocleavage furrow formation, but not for actin caps. Cellularization also requires distinct machinery to polymerize/disassemble apical microvilli and to recruit and modulate actin at the cellularization front. For transitions to occur smoothly, two fundamental changes have to occur: the location at which actin polymerization occurs must change, and a different constellation of actin regulators must be deployed to produce the distinct actin structures observed.

Our data support a hypothesis in which the balance of activity of different actin regulators at distinct sites is tightly regulated, influencing the nature of the actin structures produced. One regulator is Abl. In its absence, Ena localizes ectopically to the cortical region, upsetting the temporal and spatial balance of actin regulators (Fig. 10 B). This leads to a change in both the location and nature of actin polymerization during mitosis. Excess actin is polymerized into mi-

crovillar projections that extend from the apical region of the furrows, whereas insufficient actin is directed to the pseudocleavage furrows. Similarly, during cellularization in abl^M mutants, actin polymerization continues to be directed to apical microvilli, whereas in a wild-type embryo this ceases early in cellularization.

Our data also suggest that there is cross-talk between different modulators of actin polymerization, and that the balance of their activities determines the outcome. Although many actin modulators are unaffected in abl^M mutants, both the Arp2/3 complex and Dia are recruited to sites of ectopic actin polymerization. However, our genetic analysis suggests that although Ena mislocalization plays a critical role in the actin alterations seen in abl^M mutants, Dia and Arp2/3 mislocalization may not (Table I). In fact, reduction of the dose of Dia enhanced the abl^M phenotype. Dia normally promotes actin polymerization lining the furrows (Afshar et al., 2000). In abl^M mutants, the balance of actin polymerization is already shifted to the apical microvilli because of ectopic Ena localization. Reduction in the dose of Dia might further reduce actin polymerization in pseudocleavage furrows, resulting in the observed enhancement of the abl^M phenotype. The abnormal recruitment of Dia to the apical regions in abl^M mutants may also reduce pseudocleavage furrow formation.

It will now be important to investigate how the cell regulates the distinct types of actin polymerization required for distinct cellular and developmental processes. One mechanism of cross-talk may involve direct or indirect recruitment of one type of actin modulator by another. Abl's ability to interact with both Ena and the Arp2/3 regulator WAVE1 (for review see Woodring et al., 2003) is interesting in this regard. However, the recruitment of Arp3 and Dia to ectopic actin structures we observed in abl^M mutants may have a more simple explanation. Both are thought to have a higher affinity for newly polymerized, ATP-bound actin (for review see Pollard and Borisy, 2003), which is likely to be increased where ectopic actin polymerization appears to occur.

Relevance to Abl's action in other contexts

Drosophila Abl also functions in other contexts. It has a role in embryonic morphogenesis (Grevengoed et al., 2001), where it also acts, at least in part, via Ena. However, in this context Abl also affects AJ stability. As Ena is normally highly enriched in AJs, we hypothesize that Abl helps restrict Ena localization to AJs, and thus helps initiate the proper organization of actin underlying AJs. In Abl's absence, Ena may localize to sites other than AJs, leading to ectopic actin polymerization at those sites and reduction in actin polymerization at AJs (analogous to the divergent effects on apical actin and pseudocleavage/cellularization furrows). As the cortical actin belt underlying the AJ plays an important role in its stability, this could explain the phenotype of *abl* mutants. A similar model may help explain the roles of Abl and Ena in axon outgrowth. The network of actin filaments in the growth cone is complex, with different types of actin in filopodia and in the body of the growth cone. By regulating Ena localization, Abl may influence the balance of the different types of actin, thus influencing growth cone motility. Likewise, in fibroblasts, where Ena/VASP proteins regulate motility (Bear et al., 2000), the Arp2/3 regulators N-WASP and WAVE localize to sites at the leading edge distinct from those where Mena is found (Nakagawa et al., 2001). Whether Abl or Arg regulate the localization of Ena/VASP family proteins in mammals remains to be determined. Likewise, it is possible that deregulation of Ena/VASP proteins underlie some of the alterations in cell behavior in Bcr-Abl–transformed lymphocytes. Experiments to test whether Ena/VASP activity is important for either mammalian Abl's normal function or for the pathogenic effects of Bcr-Abl will help answer these questions.

Materials and methods

Fly stocks and genetics

Mutations and balancer chromosomes are described at FlyBase (http://flybase.bio.indiana.edu/). abl^4 germline clones were generated by the FLP dominant female-sterile technique as in Grevengoed et al. (2001). In most experiments, females with germ lines homozygous mutant for abl^4 were crossed to males heterozygous for abl^4. In the EM experiments, the females were crossed to wild-type males. The wild-type was *yellow white*. Flies expressing the actin-binding domain of moesin fused to GFP (Kiehart et al., 2000) were provided by D. Kiehart (Duke University, Durham, NC). *abl* mutants were provided by M. Hoffmann and F. Fogerty (University of Wisconsin, Madison, WI), *sop2* mutants by L. Cooley (Yale University, New Haven, CT), and *cpb* mutants by K. Miller (Washington University, St. Louis, MO). To examine possible modification of cellularization defects of abl^M mutants, females were of the genotypes *hs-flp/+;*/+;FRT-abl/FRT-Ovo*^{D} or *hs-flp/+;+/+;FRT-abl/FRT-Ovo*^{D}, where the asterisk represents either the ena^{210}, cpb^{M143} $sop2^{Q25st}$, or dia^2 mutations or the Abl transgenes. Thus, due to experimental design, only 50% of the females have an asterisk on the second chromosome.

Antibody work

To visualize actin with phalloidin, embryos were fixed in 1:1 heptane:37% formaldehyde solution for 8 min, and vitelline membranes were removed by hand. For other antibody staining, embryos were fixed for 20 min in 1:1 4% formaldehyde in PBS-heptane solution, and vitelline membranes removed with methanol. Tissues were blocked and stained in PBS/1% goat serum/0.1% Triton X-100. Antibodies were as follows: mouse mAbs anti-tubulin (1:500; Developmental Studies Hybridoma Bank, University of Iowa, Iowa City, Iowa), anti-Ena (1:500; Developmental Studies Hybridoma Bank; donated by Greg Bashaw, University of Pennsylvania, Philadelphia, PA), anti-BP102 (1:200; Developmental Studies Hybridoma Bank), and anti-phosphotyrosine (1:1,000; Upstate Biotechnology); rabbit pAbs anti-Arm N2 (1:200), anti-Arp3 (1:50; Stevenson et al., 2002; W. Sullivan, University of California, Santa Cruz, Santa Cruz, CA), and anti-Dia (1:1,500; Afshar et al., 2000; S. Wasserman, University of California, San Diego, San Diego, CA); and rat mAb anti-a-cat (1:250; T. Uemura, Kyoto Universtiy, Kyoto, Japan). Actin was visualized using Alexa® 488 phalloidin (Molecular Probes, Inc.). DNA was visualized with DAPI (Sigma-Aldrich) or propidium iodide as in Grevengoed et al. (2001). A confocal laser-scanning microscope (model 510; Carl Zeiss MicroImaging, Inc.) was used.

For immunoblotting, wild-type and abl^M mutant embryos were collected for 6 h at 18°C. Syncytial and cellularizing embryos were visually selected and used to make whole embryo extracts that were run on SDS-PAGE and immunoblotted with antibodies to Ena, Dia, Arp3, actin, and Peanut (Pnut; the loading control).

Time-lapse microscopy

Wild-type embryos were homozygous for moesin-GFP (Kiehart et al., 2000). *abl* mutants were derived from females of the genotype *hs flp;FRT-abl*^{4} *moesin-GFP/+*. Thus, all embryos were maternally expressing GFP-moesin. Bleach-dechorionated embryos were mounted in halocarbon oil (series 700; Halocarbon Products Corporation) between a coverslip and a gas-permeable membrane (petriPERM; Sartorius Corporation). Images were captured every 15 s using a Wallac Ultraview Confocal Imaging System (PerkinElmer), and image analysis was performed with either the Ultraview Software or NIH image 1.62.

Image acquisition details

All images were acquired with a confocal microscope (model 510; Carl Zeiss MicroImaging, Inc.), using LSM 510 AIM acquisition software. Both 40× (Plan-NeoFluar; NA 1.3) and 63× (Plan-Apochromat; NA 1.4) objectives were used. Embryos were mounted in Aqua Polymount (Polysciences, Inc.), and the secondary antibodies used were Alexa® 488, Alexa® 568,

Cy3, and Cy5. Adobe Photoshop® 7.0 was used to enhance brightness and contrast of images. Modifications were made on the entire panel. Care was taken to ensure that brightness and contrast alterations were performed identically on comparable wild-type and abl^{M} mutant images.

Electron microscopy

Electron microscopy was performed as in Cox et al. (1996).

Online supplemental material

Time-lapse videos supplement Fig. 4 (Videos 1 and 2) and Fig. 7 (Videos 3 and 4). Videos play at 10 frames/s. Table S1 contains a more complete data set for the fluorescence quantitations presented in Fig. 5, Fig. 6, and Fig. 8. The online supplemental material is available at http://www.jcb.org/cgi/content/full/jcb.200307026/DC1.

We are grateful to J. Carson and T. Gambling for advice and assistance with scanning EM; to J. Molk and K. Bloom for advice on fluorescence quantitation; to M. Hoffmann, G. Bashaw, L. Cooley, F. Fogerty, D. Kiehart, K. Miller, W. Sullivan, T. Uemura, S. Wasserman, the Bloomington *Drosophila* Stock Center, and the Developmental Studies Hybridoma Bank for reagents; and to B. Duronio, V. Bautch, and members of the Peifer lab for comments on the manuscript.

This work was supported by a National Institutes of Health (NIH) grant R01 GM47857 (to M. Peifer). E.E. Grevengoed was supported by NIH grants 5T32GM07092 and 1T32CA72319, J. Gates was supported by NIH grant 1F32GM068337, and M. Peifer was supported in part by a Department of Defense Breast Cancer Program Career Development Award and the Welsh Distinguished Term Professorship.

Submitted: 7 July 2003
Accepted: 4 November 2003

References

Afshar, K., B. Stuart, and S.A. Wasserman. 2000. Functional analysis of the *Drosophila* diaphanous FH protein in early embryonic development. *Development.* 127:1887–1897.

Ahern-Djamali, S.M., C. Bachmann, P. Hua, S.K. Reddy, A.S. Kastenmeier, U. Walter, and F.M. Hoffmann. 1999. Identification of profilin and src homology 3 domains as binding partners for *Drosophila* enabled. *Proc. Natl. Acad. Sci. USA.* 96:4977–4982.

Baum, B., and N. Perrimon. 2001. Spatial control of the actin cytoskeleton in *Drosophila* epithelial cells. *Nat. Cell Biol.* 3:883–890.

Bear, J.E., J.J. Loureiro, I. Libova, R. Fassler, J. Wehland, and F.B. Gertler. 2000. Negative regulation of fibroblast motility by Ena/VASP proteins. *Cell.* 101: 717–728.

Bear, J.E., T.M. Svitkina, M. Krause, D.A. Schafer, J.J. Loureiro, G.A. Strasser, I.V. Maly, O.Y. Chaga, J.A. Cooper, G.G. Borisy, and F.B. Gertler. 2002. Antagonism between Ena/VASP proteins and actin filament capping regulates fibroblast motility. *Cell.* 109:509–521.

Bennett, R.L., and F.M. Hoffmann. 1992. Increased levels of the *Drosophila* Abelson tyrosine kinase in nerves and muscles: subcellular localization and mutant phenotypes imply a role in cell-cell interactions. *Development.* 116:953–966.

Comer, A.R., S.M. Ahern-Djamali, J.-L. Juang, P.D. Jackson, and F.M. Hoffmann. 1998. Phosphorylation of Enabled by the *Drosophila* Abelson tyrosine kinase regulates the in vivo function and protein-protein interactions of Enabled. *Mol. Cell. Biol.* 18:152–160.

Cox, R.T., C. Kirkpatrick, and M. Peifer. 1996. Armadillo is required for adherens junction assembly, cell polarity, and morphogenesis during *Drosophila* embryogenesis. *J. Cell Biol.* 134:133–148.

Foe, V.E., G.M. Odell, and B.A. Edgar. 1993. Mitosis and morphogenesis in the *Drosophila* embryo: point and counterpoint. *In* The Development of *Drosophila*. Vol. 1. M. Bate and A. Martinez-Arias, editors. Cold Spring Harbor Laboratory Press, Cold Spring Harbor, NY. 149–300.

Gertler, F., J. Doctor, and F. Hoffman. 1990. Genetic suppression of mutations in the *Drosophila abl* proto-oncogene homolog. *Science.* 248:857–860.

Grevengoed, E., J. Loureiro, T. Jesse, and M. Peifer. 2001. Abelson kinase regulates epithelial morphogenesis in *Drosophila*. *J. Cell Biol.* 155:1185–1197.

Henkemeyer, M., S. West, F. Gertler, and F. Hoffmann. 1990. A novel tyrosine kinase-independent function of *Drosophila* abl correlates with proper subcellular localization. *Cell.* 63:949–960.

Hirano, S., N. Kimoto, Y. Shimoyama, S. Hirohashi, and M. Takeichi. 1992. Identification of a neural α-catenin as a key regulator of cadherin function and multicellular organization. *Cell.* 70:293–301.

Hopmann, R., J.A. Cooper, and K.G. Miller. 1996. Actin organization, bristle morphology, and viability are affected by actin capping protein mutations in *Drosophila*. *J. Cell Biol.* 133:1293–1305.

Howe, A.K., B.P. Hogan, and R.L. Juliano. 2002. Regulation of vasodilator-stimulated phosphoprotein phosphorylation and interaction with Abl by protein kinase A and cell adhesion. *J. Biol. Chem.* 277:38121–38126.

Hudson, A.M., and L. Cooley. 2002. A subset of dynamic actin rearrangements in *Drosophila* requires the Arp2/3 complex. *J. Cell Biol.* 156:677–687.

Hunter, C., and E. Wieschaus. 2000. Regulated expression of nullo is required for the formation of distinct apical and basal adherens junctions in the *Drosophila* blastoderm. *J. Cell Biol.* 150:391–401.

Kiehart, D.P., C.G. Galbraith, K.A. Edwards, W.L. Rickoll, and R.A. Montague. 2000. Multiple forces contribute to cell sheet morphogenesis for dorsal closure in *Drosophila*. *J. Cell Biol.* 149:471–490.

Koleske, A.J., A.M. Gifford, M.L. Scott, M. Nee, R.T. Bronson, K.A. Miczek, and D. Baltimore. 1998. Essential roles for the Abl and Arg tyrosine kinases in neurulation. *Neuron.* 21:1259–1272.

Korey, C.A., and D. Van Vactor. 2000. From the growth cone surface to the cytoskeleton: one journey, many paths. *J. Neurobiol.* 44:184–193.

Krause, M., J.E. Bear, J.J. Loureiro, and F.B. Gertler. 2002. The Ena/VASP enigma. *J. Cell Sci.* 115:4721–4726.

Lambrechts, A., A.V. Kwiatkowski, L.M. Lanier, J.E. Bear, J. Vandekerckhove, C. Ampe, and F.B. Gertler. 2000. cAMP-dependent protein kinase phosphorylation of EVL, a Mena/VASP relative, regulates its interaction with actin and SH3 domains. *J. Biol. Chem.* 275:36143–36151.

Lanier, L.M., and F.B. Gertler. 2000. From Abl to actin: Abl tyrosine kinase and associated proteins in growth cone motility. *Curr. Opin. Neurobiol.* 10:80–87.

Lanier, L.M., M.A. Gates, W. Witke, A.S. Menzies, A.M. Wehman, J.D. Macklis, D. Kwiatkowski, P. Soriano, and F.B. Gertler. 1999. Mena is required for neurulation and commissure formation. *Neuron.* 22:313–325.

McCartney, B.M., D.G. McEwen, E. Grevengoed, P. Maddox, A. Bejsovec, and M. Peifer. 2001. *Drosophila* APC2 and Armadillo participate in tethering mitotic spindles to cortical actin. *Nat. Cell Biol.* 3:933–938.

Nakagawa, H., H. Miki, M. Ito, K. Ohashi, T. Takenawa, and S. Miyamoto. 2001. N-WASP, WAVE and Mena play different roles in the organization of actin cytoskeleton in lamellipodia. *J. Cell Sci.* 114:1555–1565.

Plattner, R., L. Kadlec, K.A. DeMali, A. Kazlauskas, and A.M. Pendergast. 1999. c-Abl is activated by growth factors and Src family kinases and has a role in the cellular response to PDGF. *Genes Dev.* 13:2400–2411.

Pollard, T.D., and G.G. Borisy. 2003. Cellular motility driven by assembly and disassembly of actin filaments. *Cell.* 112:453–465.

Stevenson, V., A. Hudson, L. Cooley, and W.E. Theurkauf. 2002. Arp2/3-dependent pseudocleavage furrow assembly in syncytial *Drosophila* embryos. *Curr. Biol.* 12:705–711.

Sullivan, W., and W.E. Theurkauf. 1995. The cytoskeleton and morphogenesis of the early *Drosophila* embryo. *Curr. Opin. Cell Biol.* 7:18–22.

Tani, K., S. Sato, T. Sukezane, H. Kojima, H. Hirose, H. Hanafusa, and T. Shishido. 2003. Abl interactor 1 promotes tyrosine 296 phosphorylation of mammalian Enabled (Mena) by c-Abl kinase. *J. Biol. Chem.* 278:21685–21692.

Thomas, G.H., and J.A. Williams. 1999. Dynamic rearrangement of the spectrin membrane skeleton during the generation of epithelial polarity in *Drosophila*. *J. Cell Sci.* 112:2843–2852.

Turner, F.R., and A.P. Mahowald. 1979. Scanning electron microscopy of *Drosophila melanogaster* embryogenesis. III. Formation of the head and caudal segments. *Dev. Biol.* 68:96–109.

van Etten, R.A. 1999. Cycling, stressed-out and nervous: cellular functions of c-Abl. *Trends Cell Biol.* 9:179–186.

van Etten, R.A., P.K. Jackson, D. Baltimore, M.C. Sanders, P.T. Matsudeira, and P. Janmey. 1994. The COOH terminus of the c-Abl tyrosine kinase contains distinct F- and G-actin binding domains with bundling activity. *J. Cell Biol.* 124:325–340.

Vasioukhin, V., C. Bauer, M. Yin, and E. Fuchs. 2000. Directed actin polymerization is the driving force for epithelial cell-cell adhesion. *Cell.* 100:209–219.

Wang, J.Y. 2000. Regulation of cell death by the Abl tyrosine kinase. *Oncogene.* 19: 5643–5650.

Wang, Y., A.L. Miller, M.S. Mooseker, and A.J. Koleske. 2001. The Abl-related gene (Arg) nonreceptor tyrosine kinase uses two F-actin-binding domains to bundle F-actin. *Proc. Natl. Acad. Sci. USA.* 98:14865–14870.

Woodring, P.J., T. Hunter, and J.Y. Wang. 2003. Regulation of F-actin-dependent processes by the Abl family of tyrosine kinases. *J. Cell Sci.* 116:2613–2626.

Woodring, P.J., E.D. Litwack, D.D. O'Leary, G.R. Lucero, J.Y. Wang, and T. Hunter. 2002. Modulation of the F-actin cytoskeleton by c-Abl tyrosine kinase in cell spreading and neurite extension. *J. Cell Biol.* 156:879–892.